

*Intramolecular Charge Transfer (ICT) of A Chiroptically-Active Conjugated Polymer Showing Green Colour (including the correction)*

*By Hirotsugu Kawashima, Kohsuke Kawabata, Hiromasa Goto\**

*Journal of Materials Chemistry C, 3, 1126–1133, 1142 (2015).*

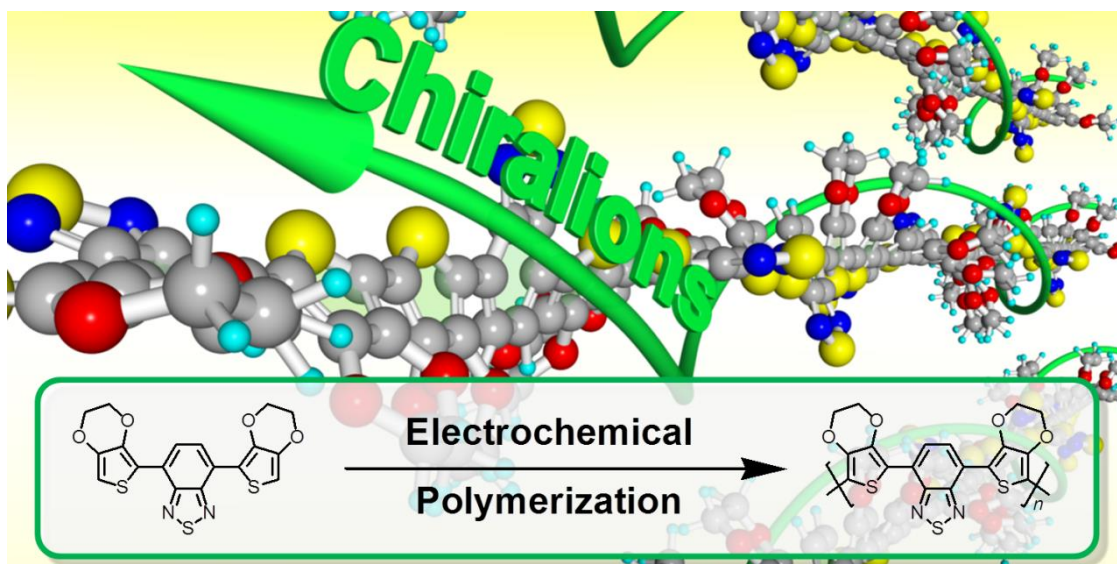
## **Intramolecular Charge Transfer (ICT) of A Chiroptically-Active Conjugated Polymer Showing Green Colour**

Hirotsugu Kawashima, Kohsuke Kawabata, Hiromasa Goto\*

Division of Materials Science, Faculty of Pure and Applied Sciences, University of Tsukuba, Tsukuba, Ibaraki 305-8573, Japan

Correspondence to H. Goto, e-mail: gotoh@ims.tsukuba.ac.jp Fax: +81-298-53-4490

### **Table of contents entry**



An optically-active, green-coloured  $\pi$ -conjugated polymer film was prepared by electrochemical synthesis in a chiral liquid crystalline media, and charge carriers are generated in the chiral conjugated system.

### **Abstract**

A donor-acceptor type achiral monomer 4,7-bis(2,3-dihydrothieno[3,4-b]-1,4-dioxin-5-yl)-2,1,3-benzothiadiazole was synthesised and electrochemically polymerised in a cholesteric liquid crystalline (CLC) medium. This film exhibits fingerprint pattern under the polarised optical microscopic observation. A possible mechanism of the fingerprint structure formation through a procedure of electrochemical polymerisation in a CLC medium is presented. Preparation of chiral polymer films even from achiral monomers is demonstrated. The film shows green colour in the reduced state and blue in

the oxidised state. Change in colour and CD signals of the film are repeatable with electrochemical oxidation and reduction. The presence of radical cations in the chiral environment, referred to as chiralions, distributed along chiral polymer chains is proposed.

## **1 Introduction**

Conjugated polymers have attracted much attention because of their characteristic optical, electrochemical and magnetic properties.<sup>1–4</sup> Applications of these materials in photovoltaic cells,<sup>5,6</sup> light-emitting diodes,<sup>7</sup> organic field-effect transistors,<sup>8</sup> and opto-electronic devices<sup>9–11</sup> have motivated development of synthesis and processing methods for conjugated polymeric materials. Electronic characters of these materials are primarily governed by the nature of the molecular conjugation. In addition, intramolecular and intermolecular interactions exert considerable influences on the properties.<sup>12,13</sup> Higher-order structures of organic materials are dependent on these interactions and molecular shapes. Precise molecular design can lead to desirable, highly-ordered structures for various applications. Therefore, micro or mesostructural control of the materials is one of the key issues for obtaining desired performance.

Liquid crystals (LCs) are considered mesophases between solid and liquid states. LCs have both fluidity and crystallinity; LC molecules can flow like a liquid, but are oriented like solid crystals at a mesoscopic level.<sup>14–16</sup> Cholesteric liquid crystalline (CLC) state is one of the chiral liquid crystalline states with a helical structure. This CLC state exhibits a twist between the individual molecules perpendicular to the director (a vector of molecular orientation). Assimilation of the asymmetric packing of CLC molecular affords formation of longer-range helical chiral structure.<sup>17,18</sup> It is known that some insects such as golden beetles and jewel beetles have this kind of periodic, anisotropic structure on their body surface.<sup>19</sup> Hariyama et al. implies that the photonic insects use such structures for recognition of their sex.<sup>20</sup> Thus, the mesoscopic structures of CLC are involved in biological activity and in some biomimetic technologies.<sup>21</sup>

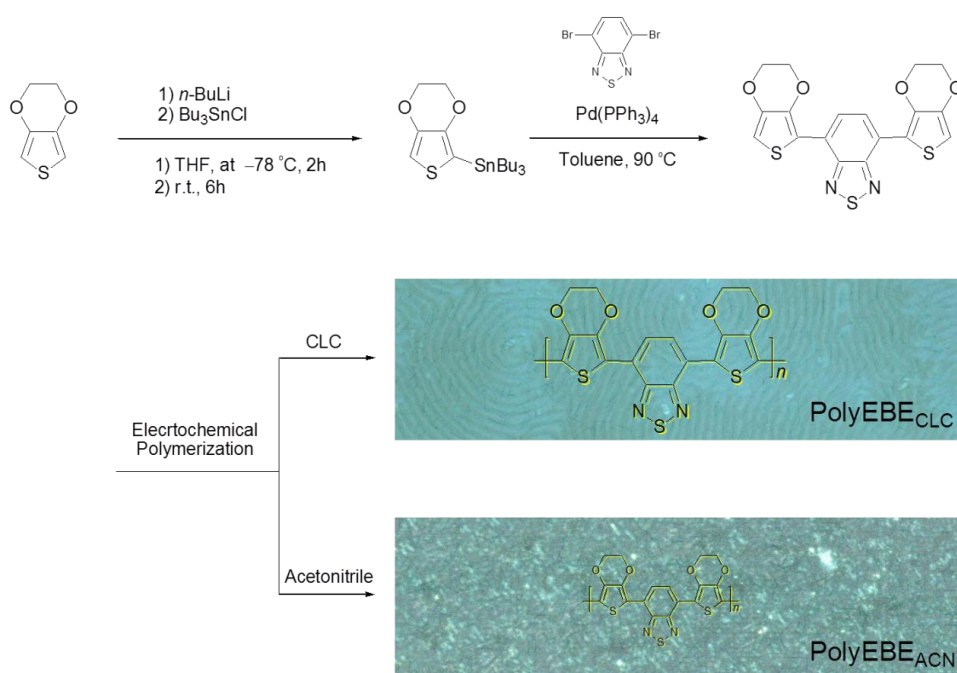
Electrochemical polymerisation is one of the methods to produce conjugated polymer films deposited directly on the electrodes.<sup>22–24</sup> Monomers in electrolytic solution are oxidised with application of potential. Then, radicals are generated on active sites of the monomers at the molecular level. Subsequently, radical polymerisation of the monomers proceeds on the electrode. Polymer films are thus deposited on the electrodes during polymerisation. Polymer films prepared by electrochemical polymerisation can be purified easily by washing with water and organic solvent. Resultant films can be used for electro-optical devices such as electrolytic capacitors and display devices.<sup>25–27</sup>

The geometric structure of polymer films prepared by electrochemical polymerisation depends strongly on the conditions of the electrolytic solution and electrode surfaces.<sup>28,29</sup>

Precise control of the conditions leads to favourable structures –regular, and highly ordered.<sup>30,31</sup> Employment of CLC as a solvent of electrochemical polymerisation, in place of isotropic liquid solvents such as acetonitrile, allows us to transcribe the fingerprint texture of a CLC medium to a resulting film.<sup>32–34</sup> Textures of the film surfaces reflect CLC's properties both structurally and optically, except that the textures are no longer flowing. Therefore, electrochemical polymerisation in a liquid crystalline medium can control meso- or macroscopic structures of resultant polymer films.<sup>35</sup>

One of the important advantages of this method is to generate chiroptically active polymer films even from achiral monomers. In this research, we prepared an achiral monomer 4,7-bis(2,3-dihydrothieno[3,4-*b*]-1,4-dioxin-5-yl)-2,1,3-benzothiadiazole (EBE), consisting of electron-donor/acceptor chemical structure, as shown in Scheme 1. Benzothiadiazole, as an electron acceptor, is sandwiched between two 2,3-dihydrothieno[3,4-*b*][1,4]dioxines (EDOTs), serving as electron donors. The low oxidation potential of EDOT units allows polymerisation in appropriate conditions.<sup>36</sup> Rod-like structures like EBE can show good affinity with LCs, because LCs consist of rod-like molecules.<sup>37</sup> Therefore, EBE can be a suitable monomer for electrochemical polymerisation in a CLC medium.

Levent et al. previously demonstrated that a polymer resulting from EBE by electrochemical polymerisation exhibited green colour in the reduced state.<sup>38,39</sup> Green colour polymers are required for green pixels of full-colour electrochromic displays. Production of green polymer requires appropriate molecular design.<sup>40–44</sup> The absorption band of green polymers is in the blue



Scheme 1. Synthetic routes to polyEBE<sub>CLC</sub> and polyEBE<sub>ACN</sub>.

and red range, with green light reflected. Our motivation in this study is to create low-bandgap, highly sensitive, and optically active polymer films for realisation of full-colour chiral electrochromic displays.

## **2 Experimental section**

### **Materials and Methods**

Chemicals were purchased from Tokyo Kasei Japan (TCI) and Merck. The reagents were used as received. ITO-coated glass ( $9 \Omega/\text{cm}^2$ ) was purchased from Furuuchi Chemical Corporation.  $^1\text{H}$  NMR spectroscopy measurements were performed in  $\text{CDCl}_3$  with an ECS 400 spectrometer (JEOL). Chemical shifts are reported in ppm downfield from  $\text{SiMe}_4$  as an internal reference. Optical texture observations were carried out using a ECLIPS LV 100 high-resolution polarizing microscope (Nikon) with a LU Plan Fluor lens and a CFIUW lens (Nikon). Digital pictures were recorded by Optio RZ10 (Pentax). FTIR absorption spectra were obtained with an FT/IR-300 spectrometer (Jasco) with the KBr method. UV-vis absorption spectra were recorded on a V-630 UV-vis optical absorption spectrometer (Jasco). Electrochemical measurements were performed using an electrochemical analyzer, PGSTAT 12 (AUTOLAB). CD spectra were obtained with a J-720 spectrometer (Jasco).

### **Synthesis of tributyl(2,3-dihydrothieno[3,4-*b*][1,4]dioxin-5-yl)stannane**

This compound was prepared by the previously reported method.<sup>45</sup> Quantities used; 2,3-dihydrothieno[3,4-*b*][1,4]dioxine (10.2 g, 71.4 mmol), tributylstannyl chloride (19.0 mL, 70.0 mmol), *n*-butyllithium (26.0 mL, 70.2 mmol), tetrahydrofuran (80 mL), a colourless oil (4.93 g, 11.4 mmol, 16.3%).  $^1\text{H}$  NMR (400 MHz,  $\delta$  from TMS (ppm),  $\text{CDCl}_3$ ):  $\delta$  0.89 (t, 9H,  $-\text{Sn}-(\text{CH}_2)_3-\text{CH}_3$ ,  $J = 7.2$  Hz), 1.09 (m, 6H,  $-\text{Sn}-(\text{CH}_2)_2-\text{CH}_2-\text{CH}_3$ ), 1.32 (m, 6H,  $-\text{Sn}-\text{CH}_2-\text{CH}_2-\text{CH}_2-\text{CH}_3$ ), 1.55 (t, 6H,  $-\text{Sn}-\text{CH}_2-\text{C}_3\text{H}_7$ ,  $J = 8.0$  Hz), 4.16 (s, 4H,  $-\text{O}-\text{CH}_2-\text{CH}_2-\text{O}-$ ), 6.57 (s, 1H, 2H (thiophene)).

### **Synthesis of 4,7-bis(2,3-dihydrothieno[3,4-*b*]-1,4-dioxin-5-yl)-2,1,3-benzothiadiazole (EBE)**

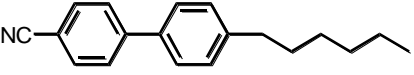
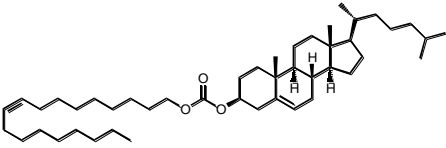
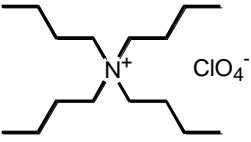
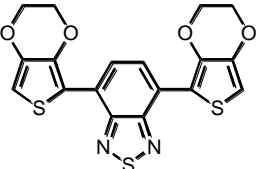
A solution of tributyl(2,3-dihydrothieno[3,4-*b*][1,4]dioxin-5-yl)stannane (285.6 mg, 0.66 mmol) and 4,7-dibromo-2,1,3-benzothiadiazole (101.9 mg, 0.37 mmol) in toluene (2 mL) is stirred for 30 min at 50 °C. Then, tetrakis(triphenylphosphine)palladium(0) (19.9 mg, 0.017 mmol) was added to the solution and refluxed for 1 day at 90 °C. After cooling, the mixture was washed with water, extracted by dichloromethane, and dried over  $\text{MgSO}_4$ . After filtration, the solvent was removed in vacuo and the crude material was purified by column chromatography (silica gel, ethyl acetate: *n*-hexane = 2:1). The product was dried in vacuo and isolated as a deep red solid (65.4 mg, 47.4%)  $^1\text{H}$  NMR (400 MHz,  $\delta$  from TMS (ppm),  $\text{CDCl}_3$ ):  $\delta$  4.33 (m, 4H,

-O-CH<sub>2</sub>-CH<sub>2</sub>-O- (outer)), 4.40 (m, 4H, -O-CH<sub>2</sub>-CH<sub>2</sub>-O- (inner)), 6.57 (s, 2H, 2H (thiophene)), 8.39 (s, 2H, 5,6H (benzene)).

### 3 Results and discussion

Constituents of the LC electrolytic solution for the reaction mixture for electrochemical polymerisation of EBE in a CLC are summarised in Table 1 (EBE, 0.89 wt%; 4-cyano-4'-n-hexylbiphenyl (6CB), 89.3 wt%; cholesterol oleyl carbonate (COC), 8.93 wt%; and tetrabutylammonium perchlorate (TBAP), 0.89 wt% as a supporting electrolyte salt). 6CB, which exhibits liquid crystallinity at room temperature, is employed as an achiral liquid crystalline molecule. Addition of a small amount of a chiral compound as a chiral inducer to a nematic liquid crystal induces cholesteric liquid crystal phase with structural chirality from achiral nematic phase.<sup>46</sup>

Table 1. Contents of reaction mixture.

Reagent	Chemical structure	wt%
4-Cyano-4'-n-hexylbiphenyl (6CB, liquid crystal)		89.3
Cholesteric oleyl carbonate (chiral inducer)		8.9
Tetrabutylammonium perchlorate (supporting electrolyte salt)		0.9
EBE (monomer)		0.9

The polymerisation process is summarised in Figure 1. This reaction mixture was charged between transparent indium-tin-oxide (ITO) coated glasses, as an anode and a cathode (Figure 1a). Visual inspection of the cell indicates formation of LC phase at room temperature (Figure 1b). Then, a DC potential of 4.0 volts was applied across the cell and the polymerisation reaction was initiated for 30 min. Colour change of the cell indicates progress of the polymerisation (Figure 1c). The rest reaction mixture on the electrode (anode side) after the polymerisation was removed by washing with *n*-hexane (Figure 1d).

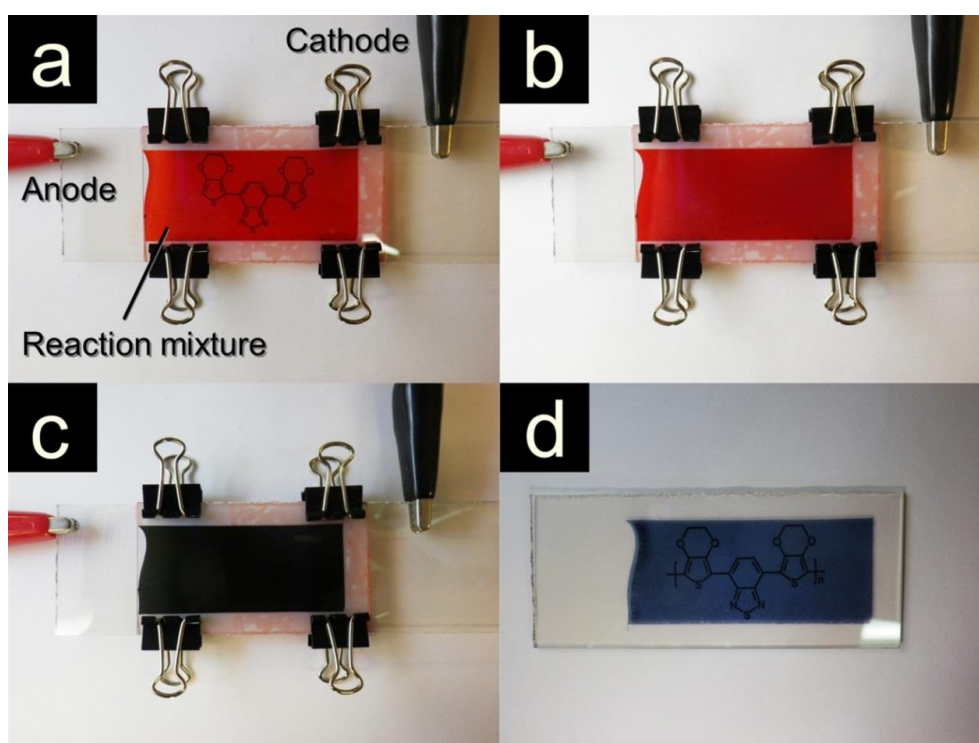


Figure 1. Polymerisation procedure of EBE in CLC electrolytic medium. a) Charge of reaction mixture (liquid phase) in a polymerisation cell. b) Phase change of the mixture from liquid to cholesteric liquid crystal. c) Colour change indicates successful progress of polymerisation. d) Resulting polymer film after washing by *n*-hexane.

Polarised optical microscopy (POM) observation reveals that the polyEBE film shows fingerprint textures, indicating transcription of CLC texture to the polymer film (Figure 2). We propose a mechanism of transcription of CLC fingerprint texture during electrochemical polymerisation in CLC medium, as illustrated in Figure 3. In a reaction mixture, monomers align along the directors of the LC before polymerisation (Figure 3b). Electrochemical polymerisation progresses on the anode surface. The polymer grows along the orientation with imprinting 3D aggregation structure of CLC. In this polymerisation process, the main chain



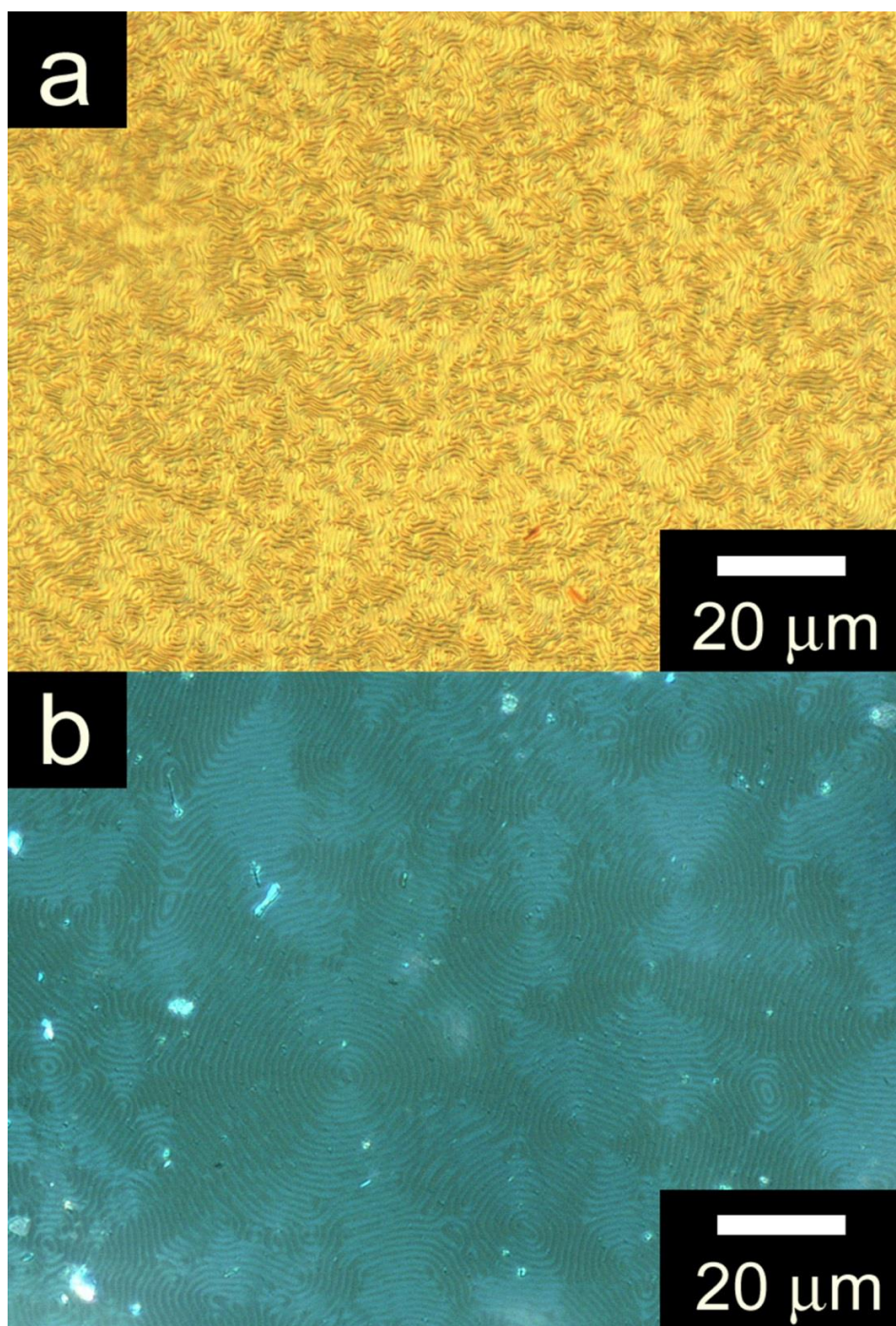


Figure 2. POM images of a) fingerprint texture of reaction mixture at room temperature, and b) transcribed fingerprint texture of polyEBE<sub>CLC</sub> at room temperature.

grows independently with phase separation against 6CB and COC (Figure 3c). Polymer film appears on the anode side in the electrochemical polymerisation. During the process, 6CB, COC can be removed during polymerisation by phase-separation process. This mechanism can be the

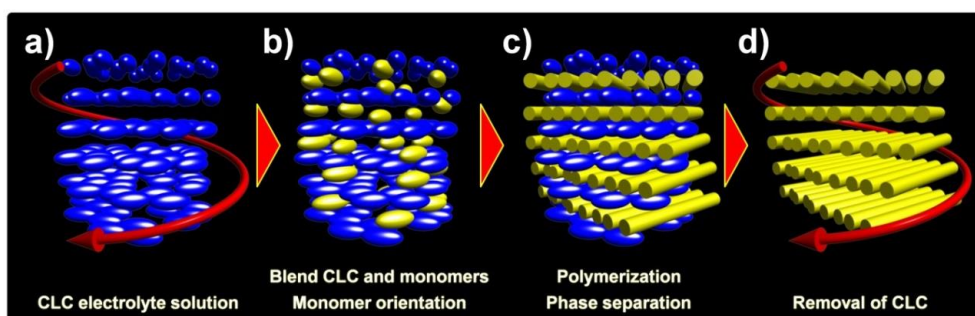


Figure 3. Illustration of mechanism of helical structure formation during electrochemical polymerisation in a CLC medium. Ellipsoids are CLC molecules (blue) and monomers (yellow); sticks are polymers.

same as Kihara et al. reported result.<sup>47</sup> Besides, washing with water and organic solvents flushes remaining 6CB, COC, TBAP and unreacted monomers from deposited polymers. The polymer thus obtained forms intermolecular twisted structure (helical structure, Figure 3d), which is similar to that of CLC. Such a process would be expected to produce fingerprint structure in the polymer.<sup>37</sup> This polymer thus prepared in CLC is abbreviated as polyEBE<sub>CLC</sub>.

Fourier transform infrared (FT-IR) absorption spectra of polyEBE<sub>CLC</sub>, EBE (monomer), 6CB liquid crystal (matrix), and COC (a chiral inducer) are shown in Figure 4. CN triple bond vibration of the matrix LC appears at 2200 cm<sup>-1</sup> for 6CB and C=O double bond vibration at 1700 cm<sup>-1</sup> for COC. PolyEBE<sub>CLC</sub> has no peaks at around 2200 cm<sup>-1</sup> and 1700 cm<sup>-1</sup> in the spectrum. Absence of these signals for polyEBE<sub>CLC</sub> in the FT-IR indicates that neither 6CB nor

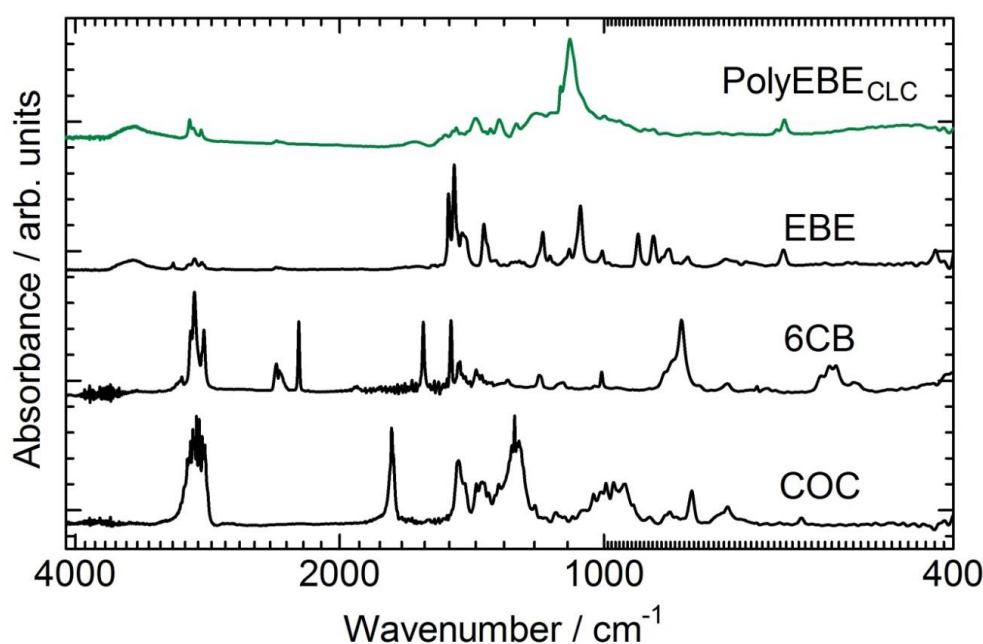


Figure 4. FT-IR absorption spectra of polyEBE<sub>CLC</sub>, EBE, 6CB and COC.



COC remain in the polyEBE<sub>CLC</sub> film. This result confirms that the fingerprint texture of the polymer is derived from pure polyEBE<sub>CLC</sub> film.

Electrochemical properties of polyEBE<sub>CLC</sub> were examined by cyclic voltammetry (Figure 5). As a reference, we additionally prepared a polyEBE film by normal electrochemical polymerisation in acetonitrile solution. This polymer is abbreviated as polyEBE<sub>ACN</sub>. Electrochemical measurements for the resultant polymer were carried out at scan rates of 10 to 100 mV/s, respectively, in acetonitrile containing 0.1 M TBAP. The potentials are estimated relative to a silver-silver ion (Ag/Ag<sup>+</sup>) reference electrode. Cyclic voltammograms of polyEBE<sub>CLC</sub> and polyEBE<sub>ACN</sub> show oxidation and reduction signals at the same position. The

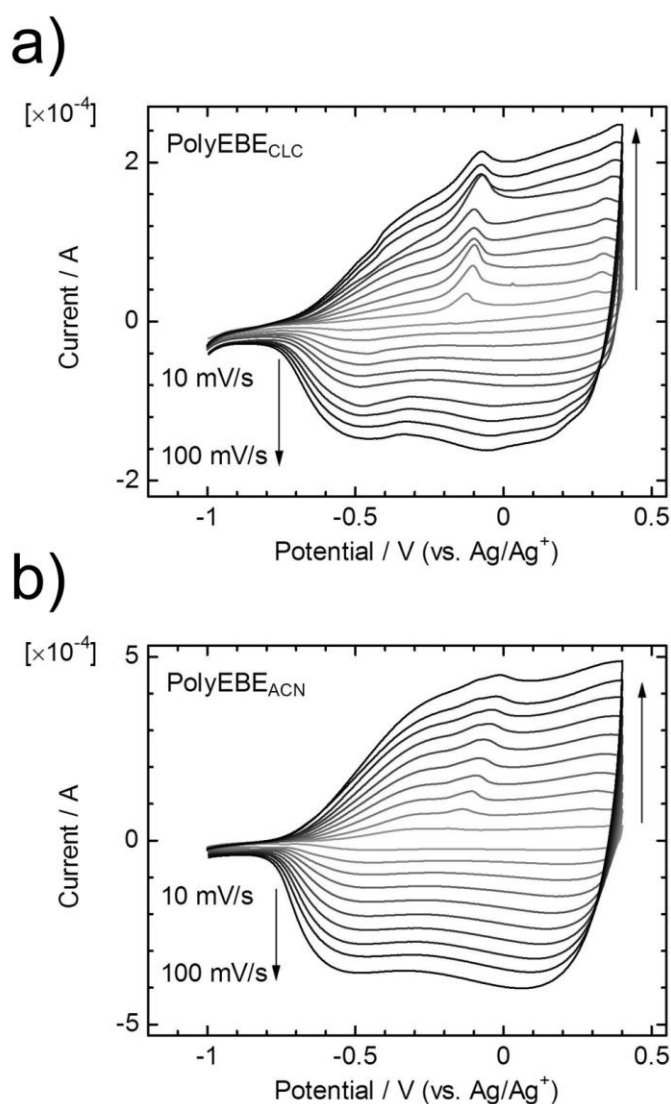


Figure 5. Cyclic voltammograms of polyEBE observed by electrochemical polymerisation. a) A polymer prepared in a cholesteric liquid crystalline medium, and 2) a polymer prepared in acetonitrile electrolytic solution.

polyEBE<sub>CLC</sub> film shows the same electrochemical response as polyEBE<sub>ACN</sub>. This reflects that the redox property depends on the primary structure of the polymers.

UV-vis absorption changes of polyEBE<sub>CLC</sub> with electrochemical oxidation and reduction were observed (Figure 6). In the reduced state, two absorption maxima appeared near 725 nm and 425 nm (Figure 6a). The 425 nm band is assignable to  $\pi-\pi^*$  transition. The 725 nm band is due to an intramolecular charge transfer (ICT) band typically observed from donor-accepter structures. The band-edge bandgap of the polymer is estimated by onset of the optical absorption to be 1.24 eV. This absorption band is changed drastically by the electrochemical redox process. In the oxidised state (Figure 6b), the two bands decrease in intensity and a polaron band (doping band) appears at long wavelengths. This change is repeatable under electrochemical redox. Electrochromism of polyEBE films was observed during the electrochemical process. The change in colour is visually confirmed, as shown in Figures 7b,d.

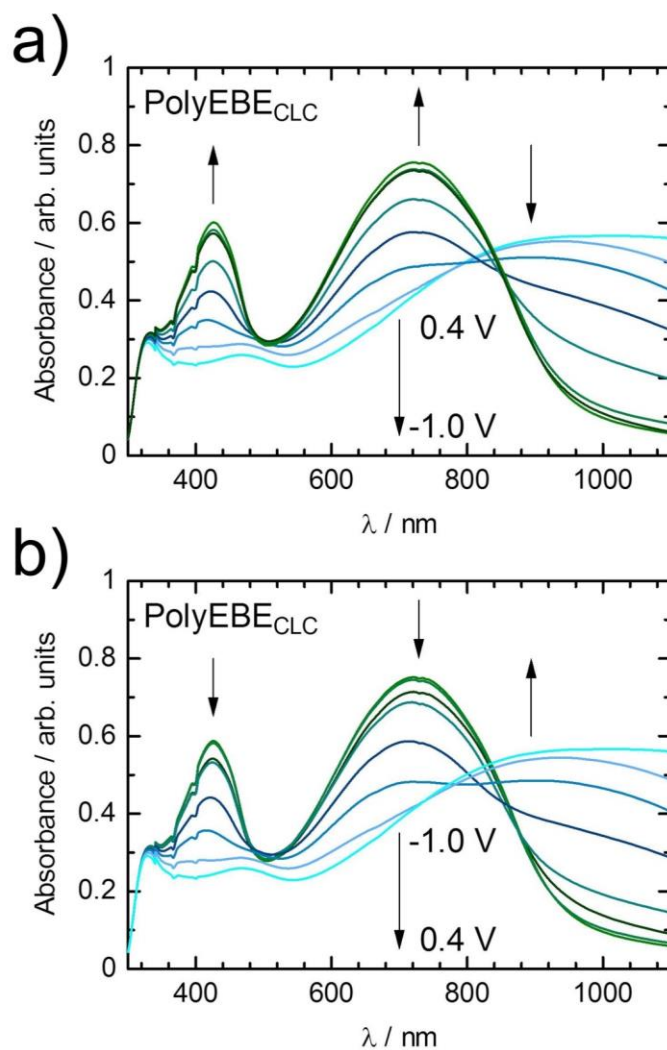


Figure 6. Changes of UV-vis absorption spectra of a polyEBE<sub>CLC</sub> film in electrochemical reduction and oxidation (vs. Ag/Ag<sup>+</sup>).

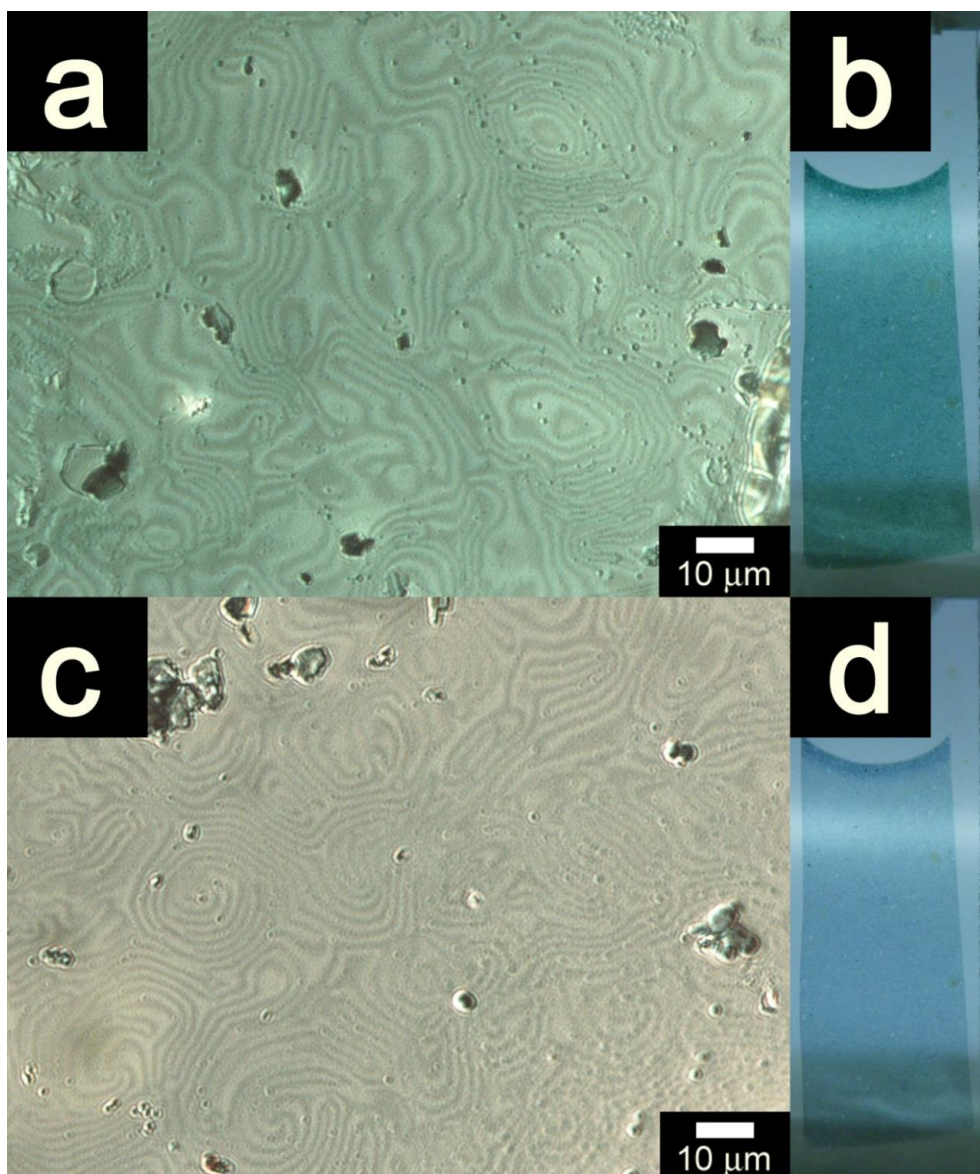


Figure 7. POM and visual observation of electrochromism of polyEBE<sub>CLC</sub> in green (a,b) and blue (c,d) colours.

The film exhibited green colour in the reduced state and blue colour in the oxidised state. This colour change is repeatable by electrochemical redox switching. The mesoscopic fingerprint structure of the film is maintained over several electrochemical redox processes (Figures 7a,c). The same UV-vis observation was demonstrated for polyEBE<sub>ACN</sub> for comparison. As shown in Figure 8, UV-vis absorption behaviour of polyEBE<sub>ACN</sub> with electrochemical redox process is identical to polyEBE<sub>CLC</sub>.

Circular dichroism (CD) of polyEBE<sub>CLC</sub> is also tunable with a electrochemical redox process, as shown in Figure 9. CD spectra of polyEBE<sub>CLC</sub> have several peaks overlapping each other

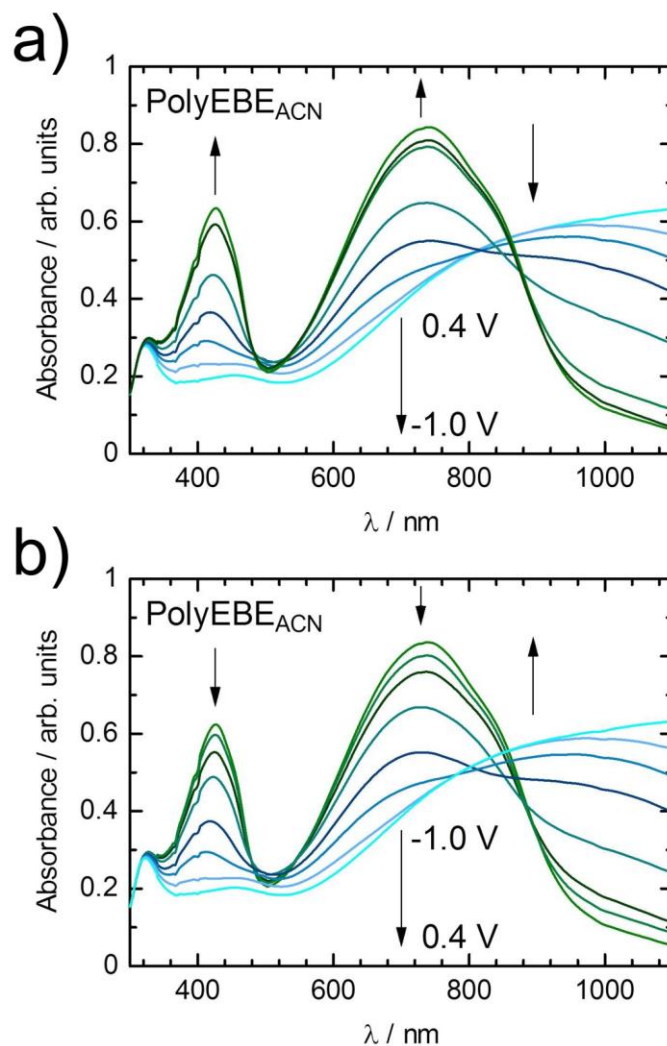


Figure 8. Changes of UV-vis absorption spectra of a polyEBE<sub>ACN</sub> film in electrochemical reduction and oxidation (vs. Ag/Ag<sup>+</sup>).

near absorption maxima. As a result, the observation showed two negative bisignate Cotton effects. These Cotton effects appear at around 720 nm and 440 nm, respectively. These values are in excellent agreement with the two peaks of UV-vis spectra (725 nm, 425 nm). Therefore, these Cotton effects can be attributed to ICT and  $\pi$ - $\pi^*$  transitions, respectively. Both the Cotton effects are strengthened from the oxidised state to the reduced state. This CD observation results indicate that polyEBE has structural chirality derived from its aggregated helical structure transcribed by CLC.

These changes of the CD spectra suggest that structural changes in the aggregation form of the helical structure may occur with the electrochemical redox process, because the optical activity of the polymer derives from structural chirality in a manner similar to CLC. Moreover, repeating changes in ellipticity at 860 nm and 410 nm in electrochemical oxidation and

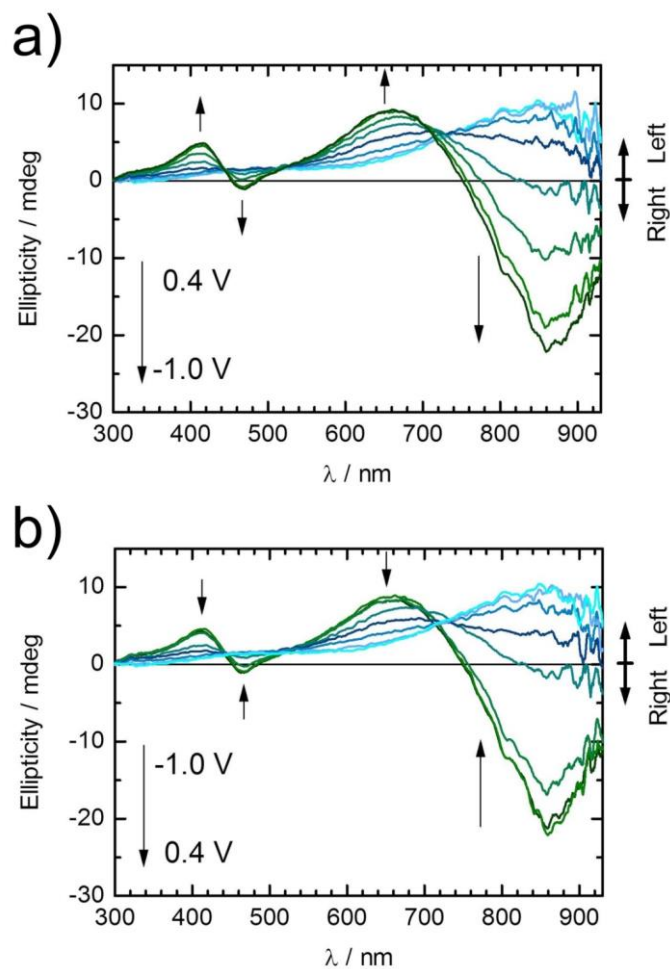


Figure 9. CD spectra of polyEBE<sub>CLC</sub> with applied voltage (vs. Ag/Ag<sup>+</sup>).

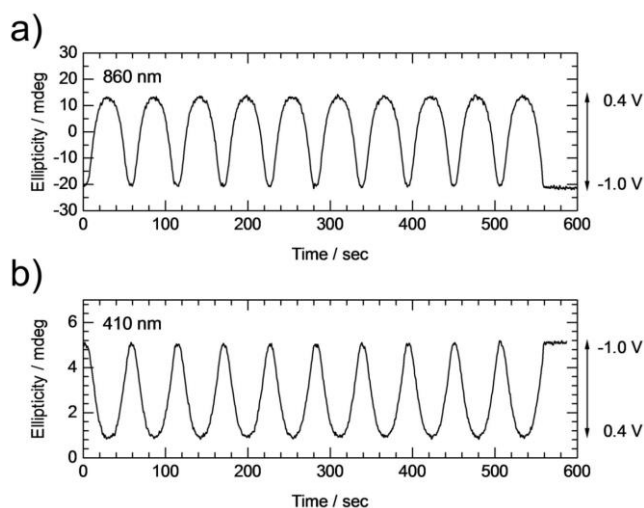


Figure 10. Repeating changes in ellipticity of polyEBE<sub>CLC</sub> at 860 nm (a) and 410 nm (b) in electrochemical oxidation and reduction. Applied voltage was cyclically swept 10 times from -1.0 V to 0.4 V at 50 mV/sec (vs. Ag/Ag<sup>+</sup>).



reduction were obtained as shown in Figure 10. Applied voltages were cyclically swept 10 times from -1.0 V to 0.4 V at 50 mV/s with automatic control by the instrument. The ellipticities were maintained completely after 10 cycles. This suggests that the polyEBE film is mechanically stable and can maintain its optical properties against applied voltage within -1.0 V to 0.4 V.

A broad UV-vis absorption band at longer wavelength region (800 nm) appeared in the oxidised state indicates generation of polarons. In this state, a pair of a radical and a cation is generated along  $\pi$ -conjugated polymer chains. This behaviour can be detected by using electron spin resonance (ESR) spectroscopy. Figure 11 shows changes in the ESR signals derived from radicals on polyEBE in the electrochemical redox processes. Both in reduction and oxidation

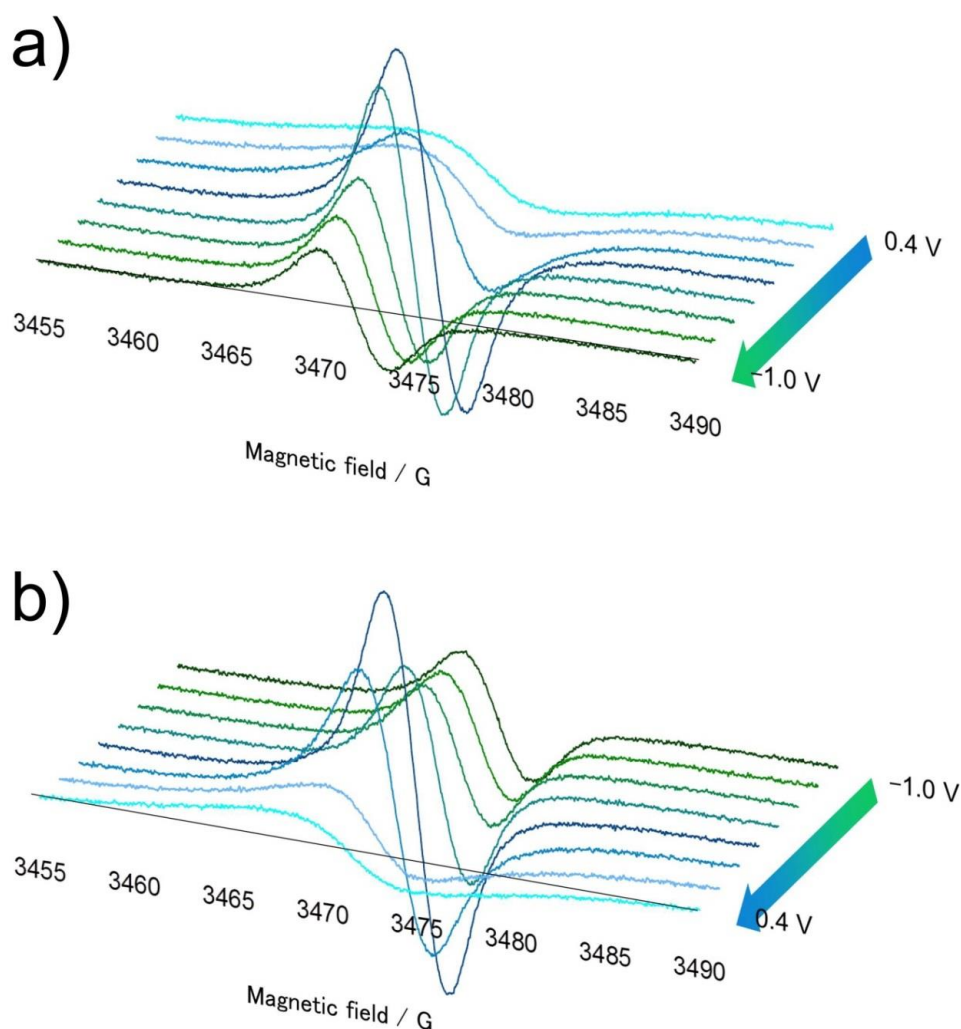


Figure 11. Changes of ESR spectra of polyEBE<sub>CLC</sub> film in electrochemical reduction (a) and oxidation (b) (vs. Ag/Ag<sup>+</sup>).

processes, the signal displays the maximum value. In the oxidation process, further electron extraction from the polaron state results in generation of bipolarons. In this state, the main charge carrier is a pair of two cations (dications) in place of radical cations. Thus, the ESR intensity is decreased from the maximum in the oxidation process due to change of species of the carrier from radical cations to dications. After the oxidation, the ESR signal was repeatedly changed in the redox. This repeated change can be performed in further cyclic sweeps, as well as change in the UV-vis and the CD.

Focusing on differences between electrochemical reduction and oxidation of polyEBE<sub>CLC</sub>, changes in  $g$ -value and peak height of ESR spectra were examined. These changes are summarised in Figure 12, exhibiting hysteresis behaviour. This hysteresis may be due to the difference in diffusion rate between intrusion and extrusion (doping-dedoping or oxidation-reduction) of ions. The same behaviour can be observed in the UV-vis absorption and the CD. Compared to those of polyEBE<sub>ACN</sub>, responsiveness to change in applied voltage is fast. This means that hysteresis in applied voltage of polyEBE<sub>CLC</sub> is smaller than that of polyEBE<sub>ACN</sub>. Difference in crystallinity of these polymer films might affect the diffusion of the ions.

PolyEBE films prepared by electrochemical polymerisation using CLC medium have ordered structure consisting of polymer chains, which is transcribed from the CLC medium. The fingerprint structure should be twisting along with the CLC order. Charge carriers such as

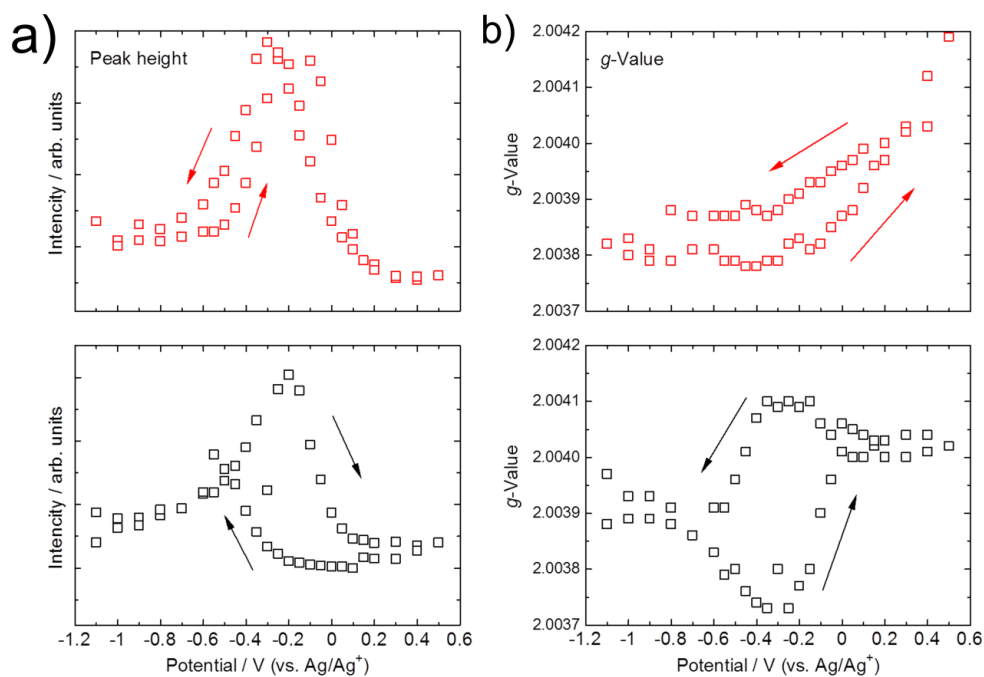


Figure 12. ESR changes of peak height (a) and  $g$ -value (b) of polyEBE<sub>CLC</sub> (above) and polyEBE<sub>ACN</sub> (below) in electrochemical reduction and oxidation.

radical cations (polarons) and dications (bipolarons) can move along the helical chains. Such charge carriers delocalised along the chiral conjugated system, referred to as “chiralions,” are observed (Figure 13).

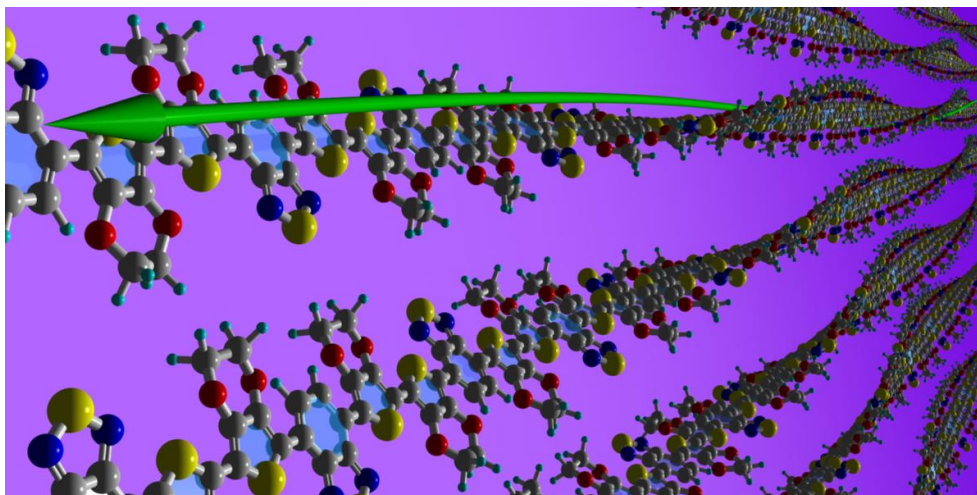


Figure 13. A graphic image of “chiralion,” a radical cation moving along the polyEBE<sub>CLC</sub> chain in helical aggregation structure.

#### 4 Conclusions

A donor-acceptor type chiral polymer film showing fingerprint surface structure was prepared successfully by electrochemical polymerisation in a cholesteric liquid crystalline medium. This polymer film appears green in the reduced state and blue in the oxidised state. Colour change and CD signals of the film are repeatable after electrochemical oxidation and reduction. Generation of charge carriers in polaron and bipolaron states was confirmed by using the ESR. Chiralions, charge carriers delocalised along the optically-active  $\pi$ -conjugated system is proposed. This polyEBE<sub>CLC</sub> may be the first example of ICT-type conjugated polymer with electro-optical activity.

**Acknowledgements.** We would like to thank the Chemical Analysis Division Research Facility Centre for Science and Technology, and Glass Work Shop, of the University of Tsukuba.

#### References

- 1 K. Wagner, R. Byrne, M. Zannoni, S. Gambhir, L. Dennany, R. Breukers, M. Higgins, P. Wagner, D. Diamond, G. G. Wallace and D. L. Officer, *J. Am. Chem. Soc.*, 2011, **133**, 5453–5462.
- 2 F. B. Koyuncu, E. Sefer, S. Koyuncu and E. Ozdemir, *Macromolecules*, 2011, **44**,

8407–8414.

- 3 E. Collini and G. D. Scholes, *Science*, 2009, **323**, 369–373.
- 4 C. M. Cardona, W. Li, A. E. Kaifer, D. Stockdale and G. C. Bazan, *Adv. Mater.*, 2011, **23**, 2367–2371.
- 5 S. Song, S. Park, S. Kwon, B. H. Lee, J. A. Kim, S. H. Park, Y. Jin, J. Lee, I. Kim, K. Lee and H. Suh, *Synth. Met.*, 2012, **162**, 1936–1943.
- 6 E. Nasybulin, S. Wei, M. Cox, I. Kymissis and K. Levon, *J. Phys. Chem. C*, 2011, **115**, 4307–4314.
- 7 M. H. Han, H. J. Song, T. H. Lee, J. Y. Lee, D. K. Moon and J. R. Haw, *Synth. Met.*, 2012, **162**, 2294–2301.
- 8 S. Ko, E. T. Hoke, L. Pandey, S. Hong, R. Mondal, C. Risko, Y. Yi, R. Noriega, M. D. McGehee, J.-L. Brédas, A. Salleo and Z. Bao, *J. Am. Chem. Soc.*, 2012, **134**, 5222–5232.
- 9 S. I. Cho, W. J. Kwon, S.-J. Choi, P. Kim, S.-A. Park, J. Kim, S. J. Son, R. Xiao, S.-H. Kim and S. B. Lee, *Adv. Mater.*, 2005, **17**, 171–175.
- 10 Y. Pang, X. Li, H. Ding, G. Shi and L. Jin, *Electrochim. Acta*, 2007, **52**, 6172–6177.
- 11 P. Taranekar, T. Fulghum, A. Baba, D. Patton and R. Advincula, *Langmuir*, 2007, **23**, 908–917.
- 12 S. S. Pinnock, C. N. Malele, J. Che and W. E. Jones Jr., *J. Fluoresc.*, 2012, **22**, 583–589.
- 13 B.-G. Kim, E. J. Jeong, H. J. Park, D. Bilby, L. J. Guo and J. Kim, *ACS Appl. Mater. Interfaces*, 2011, **3**, 674–680.
- 14 T. J. White, M. E. McConney and T. J. Bunning, *J. Mater. Chem.*, 2010, **20**, 9832–9847.
- 15 K. Rameshbabu, A. Urbas and Q. Li, *J. Phys. Chem. B*, 2011, **115**, 3409–3415.
- 16 S. N. Lee, L.-C. Chien and S. Sprunt, *Appl. Phys. Lett.*, 1998, **72**, 885–887.
- 17 G. Solladié and R. G. Zimmermann, *Angew. Chem. Int. Ed. Engl.*, 1984, **23**, 348–362.
- 18 T. J. White, R. L. Bricker, L. V. Natarajan, N. V. Tabiryan, L. Green, Q. Li and T. J. Bunning, *Adv. Funct. Mater.*, 2009, **19**, 3484–3488.
- 19 V. Sharma, M. Crne, J. O. Park and M. Srinivasarao, *Science*, 2009, **32**, 449–451.
- 20 D. G. Stavenga, B. D. Wilts, H. L. Leertouwer and T. Hariyama, *Phil. Trans. R. Soc. B*, 2011, **366**, 709–723.
- 21 S. Lowrey, L. D. Silva, I. Hodgkinson and J. Leader, *J. Opt. Soc. Am. A.*, 2007, **24**, 2418–2425.
- 22 G. A. Sotzing and J. R. Reynolds, *Chem. Mater.*, 1996, **8**, 882–889.
- 23 S. Akoudad and J. Roncali, *Synth. Met.*, 1999, **101**, 149.
- 24 P. Si, Q. Chi, Z. Li, J. Ulstrup, P. J. Møller and J. Mortensen, *J. Am. Chem. Soc.*, 2007, **129**, 3888–3896.
- 25 H. Yamamoto, M. Oshima, M. Fukuda, I. Isa and K. Yoshino, *J. power sources*, 1996, **60**,

173–177.

- 26 J. Zhang, L.-B. Kong, B. Wang, Y.-C. Luo and L. Kang, *Synth. Met.*, 2009, **159**, 260–266.
- 27 R. J. Mortimer, A. L. Dyer and J. R. Reynolds, *Displays*, 2006, **27**, 2–18.
- 28 M. C. Turhan, M. Weiser, H. Jha and S. Virtanen, *Electrochim. Acta*, 2011, **56**, 5347–5355.
- 29 M. S. Cho, Y. Y. Yun, J. D. Nam, Y. Son and Y. Lee, *Synth. Met.*, 2008, **158**, 1043–1046.
- 30 T. Hatano, A.-H. Bae, M. Takeuchi, N. Fujita, K. Kaneko, H. Ihara, M. Takafuji and S. Shinkai, *Angew. Chem.*, 2004, **116**, 471–475.
- 31 Y. H. Wijsboom, A. Patra, S. S. Zade, Y. Sheynin, M. Li, L. J. W. Shimon and M. Bendikov, *Angew. Chem. Int. Ed.*, 2009, **48**, 5443–5447.
- 32 H. Goto, *J. Mater. Chem.*, 2009, **19**, 4914–4921.
- 33 H. Yoneyama, A. Tsujimoto and H. Goto, *Macromolecules*, 2007, **40**, 5279–5283.
- 34 K. Kawabata, H. Yoneyama and H. Goto, *Mol. Cryst. Liquid Cryst.*, 2009, **515**, 3–15.
- 35 K. Kawabata, H. Yoneyama and H. Goto, *Polym. Chem.*, 2010, **1**, 1606–1608.
- 36 G. J. McEntee, P. J. Skabara, F. Vilela, S. Tierney, I. D. W. Samuel, S. Gambino, S. J. Coles, M. B. Hursthouse, R. W. Harrington and W. Clegg, *Chem. Mater.*, 2010, **22**, 3000–3008.
- 37 K. Kawabata and H. Goto, *Chem. Lett.*, 2009, **38**, 706–707.
- 38 A. Durmus, G. E. Gunbas, P. Camurlu and L. Toppare, *Chem. Commun.*, 2007, 3246–3248.
- 39 S. Tarkuc, E. K. Unver, Y. A. Udum and L. Toppare, *Eur. Polym. J.*, 2010, **46**, 2199–2205.
- 40 I. Schwendeman, R. Hickman, G. Sönmez, P. Schottland, K. Zong, D. M. Welsh and J. R. Reynolds, *Chem. Mater.*, 2002, **14**, 3118–3122.
- 41 G. Sönmez, C. K. F. Shen, Y. Rubin and F. Wudl, *Angew. Chem. Int. Ed.*, 2004, **43**, 1498–1502.
- 42 G. Sönmez, H. B. Sönmez, C. K. F. Shen, R. W. Jost, Y. Rubin and F. Wudl, *Macromolecules*, 2005, **38**, 669–675.
- 43 G. E. Gunbas, A. Durmus and L. Toppare, *Adv. Mater.*, 2008, **20**, 691–695.
- 44 W.-H. Chen, K.-L. Wang, D.-L. Liaw, K.-R. Lee and J.-Y. Lai, *Macromolecules*, 2010, **43**, 2236–2243.
- 45 S. S. Zhu and T. M. Swager, *J. Am. Chem. Soc.*, 1997, **119**, 12568–12577
- 46 G. Gottarelli, M. Hibert, B. Samori, G. Solladié, G. P. Spada and R. Zimmermann, *J. Am. Chem. Soc.*, 1983, **105**, 7318–7321.
- 47 H Kihara and T Miura, *Polymer* 2005, **46**, 10378–10382.



Correction. *J. Mater. Chem. C*, 2015, 3, 1142-1142.

Roncali *et al* previously synthesized the monomer with a Pd(II) catalyst for the Stille coupling reaction,<sup>1</sup> although the present research employed Pd(0) catalyst.

1. J.-M. Raimundo, P. Blanchard, H. Brisset, S. Akoudad and J. Roncali, *Chem. Commun.*, 2000, 939–940.